Plastics, Rubber and Composites
Macromolecular Engineering

ISSN: 1465-8011 (Print) 1743-2898 (Online) Journal homepage: https://www.tandfonline.com/loi/yprc20

Investigating the effects of processing parameters on poly(lactic acid) properties – a central composite design approach

Mohammad Reza Ketabchi, Mohammad Khalid, Chantara Thevy Ratnam, Feven Mattews Michael & Rashmi Walvekar

To cite this article: Mohammad Reza Ketabchi, Mohammad Khalid, Chantara Thevy Ratnam, Feven Mattews Michael & Rashmi Walvekar (2019): Investigating the effects of processing parameters on poly(lactic acid) properties – a central composite design approach, Plastics, Rubber and Composites

To link to this article: https://doi.org/10.1080/14658011.2019.1570444

Published online: 30 Jan 2019.

PLASTICS, RUBBER AND COMPOSITES
https://doi.org/10.1080/14658011.2019.1570444

The Institute of Materials, Minerals and Mining

Taylor & Francis
Taylor & Francis Group

Investigating the effects of processing parameters on poly(lactic acid) properties – a central composite design approach

Mohammad Reza Ketabchi[a], Mohammad Khalid[b], Chantara Thevy Ratnam[c], Feven Mattews Michael[a] and Rashmi Walvekar[d]

[a]Department of Chemical and Environmental Engineering, The University of Nottingham Malaysia Campus, Semenyih, Malaysia; [b]Graphene & Advanced 2D Materials Research Group (GAMRG), Sunway University, Subang Jaya, Malaysia; [c]Radiation Processing Technology Division, Malaysian Nuclear Agency, Bangi, Malaysia; [d]School of Engineering, Taylor's University, Subang Jaya, Malaysia

ABSTRACT

This study attempts to optimise poly(lactic acid) processing parameters using central composite design approach which is well known statistical tool in design of experiments. Three factors and five levels were chosen for carrying out the analysis. The parameters include mixing temperature (180–210°C), screw speed (50–100 rev min^{-1}) and mixing time (5–10 min), which were varied independently. The results were evaluated based on maximum stress, tensile modulus, and impact strength under different conditions and the significant factors were determined using variance analysis (ANOVA). An optimum balance between the mechanical properties was obtained when the samples were blend at 180°C at 100 rev min^{-1} rotor speed for 10 min. Moreover, validation of the predicted results confirmed the optimised parameters, which were further complemented by morphological and thermal studies.

ARTICLE HISTORY
Received 30 June 2016
Revised 24 May 2018
Accepted 11 January 2019

KEYWORDS
Poly(lactic acid); response surface methodology; optimisation; mechanical properties; thermal stability

Introduction

Increased application of synthetic packaging films has resulted in serious environmental problems following their non-biodegradability. Therefore, poly(lactic acid) (PLA) which is environmentally friendly and possess biodegradable properties has recently found many applications in industries such as food packaging. However, controlling the processing parameters such as mixing time, temperature and rotor speed that determine the overall properties of a polymer are very difficult. To overcome this drawback, it is necessary to optimise the processing parameters to obtain superior final properties for a polymer blend.

Industries (mainly food packaging) are steadily introducing environmental friendly materials to their production line [1,2]. This is due to the environmental pollution problems caused by using oil-based plastics [3,4]. Following this growing trend, bioplastics have attracted a great interest for a diverse range of applications such as their renewability, biodegradability, and commercial viability [5,6]. They are mainly classified into four categories; photodegradable bioplastics, compostable bioplastics, bio-based bioplastics and biodegradable bioplastics [7,8]. Meanwhile, PLA, a leading bioplastics member is found to be a suitable replacement for fossil-based plastics [9,10].

PLA, as a hydrophilic thermoplastic polymer, is derived from natural feedstock such as corn, barley, sugar beets, wheat and rice [11,12]. Scientists have recently improved the mechanical properties of PLA by introducing suitable plasticizers such as Polyethylene glycols (PEG) [13,14]. Addition of a plasticizer could be considered expensive, as it requires further processing optimisation. Therefore PLA was modified itself to enhance the temperature stability of the polymer and reduce the residual monomer content [15]. The modification processes for PLA are similar to the ones employed for thermoplastic polymers, which are mainly proposed to enhance thermal stability of the material.

Meanwhile, it is understood that the processing methods and parameters exhibit significant effects on the final product [16,17]. In addition to solvent casting, melt compounding/extrusion is commonly carried out to introduce PLA granules in different compositions [18–20]. Through melt compounding, the processing parameters are mainly temperature, mixing speed and time. The production lines based on PLA matrices are strictly limited during the processing procedure due to the nature of PLA. As a result of this limitation, studies mainly employed the granules at ~170°C [21–23]. This was to reduce the thermal impact on PLA as a natural feedstock derivative. The processing temperature plays important role in cases where higher temperatures are required to melt other components in the composite.

Studies showed effective outcomes using optimisation techniques such as Response Surface Methodology (RSM) [14,24]. Determination of optimum conditions, involves evaluation of several variables

CONTACT Mohammad Khalid khalids@sunway.edu.my

influence individually and their interactions concurrently. At the same time, it estimates the relation between the obtained responses and the independent variables. Compared to conventional method this technique saves a notable amount of time, energy and money by reducing and optimising the number of experiments [25]. For instance, for a standard three factorial based design, 27 experiments should be performed while using a Central Composite Design (CCD) in RSM only 20 experiments are required to be performed [26]. Despite the drop in number of experiments, similar and in most cases superior optimised outcomes were obtained.

The main focus of the results presented in this paper will be on the significance of temperature, speed and time of processing on mechanical properties of PLA. Therefore, to investigate the maximum processing temperature of pure PLA, via the least possible number of experiments, response surface methodology (RSM) was employed. Morphological studies were conducted to further understand the role of processing temperature on the morphology development of PLA.

Methodology

Materials

Polylactic acid (Ingeo biopolymer) grade 2003D (Melt index 6 g/10 min, density 1.22 g cm^{-3}) was obtained from NatureWorks LLC product, USA. Biopolymer granules were oven dried at 60°C for 12 h before blending.

Experimental design and statistical analysis

The interaction and optimisation of blending parameters such as mixing speed (rev min^{-1}) (A), mixing temperature (°C) (B) and mixing duration (min) (C) was studied using Response Surface Methodology (RSM). Table 1 presents the list of factors (blending parameters) and range of levels used. These factors are experimental variables that can be changed independently of each other. In addition, the factors were analysed based on the mechanical properties of the blended samples such as maximum stress, young modulus, and impact strength. These are the dependent variables known as the responses. Table 2 presents the set of experimental trials generated by the Design Expert software (V8) to reach maximum results with minimal number of possible experiments. The experimental trials were based on the 3 factors and 5 levels using CCD. The responses were then fitted to quadratic polynomial models. Suitability of quadratic polynomial model was then determined by regression coefficient R^2. Furthermore, *F*-value and *P*-value were used to check the regression coefficient significances. *F-value* is determined using the mean square of the pure error instead of the residual error. *P-value* is the probability of the null hypothesis.

Experimental procedure

The melt compounding of PLA granules was carried out in Brabender PL2000-6 twin-screw compounder according to the experimental design conditions (Table 2). The compounded PLA granules were then moulded into BS6746 and ASTM D256 standards using a bench top injection moulding machine (RR3400, RAY-RAN Injection Moulding Machine, United Kingdom), at 180°C and 90°C for barrel and mould temperatures, respectively. Holding time for the BS6746 and ASTM D256 samples were 4 and 8 s, respectively. All specimens were conditioned at ambient condition for 48 h before conducting any tests.

Characterisation and analysis

Tensile testing

To compare and evaluate the tensile properties of the pure PLA, the samples were moulded using BS6746 standard. The test was carried out using tensile tester, TOYOSEIKI Strograph R-1. The crosshead speed utilised was 5 mm min^{-1}. Total of 7 samples were tested and an average of 5 repeating samples was reported.

Impact testing

The impact properties of the notched pure PLA samples prepared using ASTM D256 standard were tested using CEAST Impact Pendulum Tester (Model CE UM-636), with a 4 J hammer. Total of 7 samples were tested and an average of 5 repeating samples was reported.

Interfacial morphology analysis (FESEM)

Fractured surface of the tensile and impact samples were observed with a field emission scanning electron microscope (FESEM, FEI Quanta 400 FE-SEM) under 20 kV.

Table 1. Levels of independent variables.

			Levels					
Independent variables	Codes	Type	Minimum	Maximum	−1 Actual	+1 Actual	Mean	Std. Dev.
mixing speed (rev min^{-1})	A	Numeric	50.00	100.00	50.00	100.00	75.00	17.68
mixing temperature (°C)	B	Numeric	180.00	210.00	180.00	210.00	195.00	10.61
mixing duration (min)	C	Numeric	5.00	10.00	5.00	10.00	7.50	1.77

Table 2. CCD design of three variables with their obtained responses.

Exp. name	Speed (rev min^{-1})	Temperature (°C)	Duration (min)	Max stress (MPa)	Young's Modulus (MPa)	Impact (J m^{-1})
H1	100	180	5	57.08	611.3	30.878
H2	75	195	10	55.48	582.943	30.099
H3	50	210	5	52.25	648.478	29.804
H4	75	195	7.5	56.77	527.136	28.816
H5	100	210	5	38.08	776.205	22.367
H6	75	195	7.5	56.77	527.136	28.816
H7	75	195	7.5	56.77	527.136	28.816
H8	50	195	7.5	54.04	573.646	38.474
H9	100	180	10	56.33	651.137	32.299
H10	75	195	7.5	56.77	527.136	28.816
H11	75	180	7.5	60.89	605.713	30.476
H12	75	195	7.5	56.77	527.136	28.816
H13	75	195	5	58.12	556.089	29.787
H14	50	210	10	50.64	633.474	26.016
H15	100	210	10	41.62	650.77	23.247
H16	75	195	7.5	56.77	527.136	28.816
H17	100	195	7.5	55.77	589.227	29.889
H18	50	180	10	55.56	549.23	28.175
H19	50	180	5	55.09	638.06	29.857
H20	75	210	7.5	51.39	616.953	28.285

Thermal analysis

Thermogravimetric analysis (TGA) was carried out using a Perkin Elmer simultaneous thermal analyser (STA 6000, USA) in a nitrogen atmosphere, flow rate 10 ml min^{-1} at temperature between 30°C and 500°C and heating rate of 10°C min^{-1}.

Results and discussion

Processing parameters modelling

Table 2 summarises the obtained maximum stress, impact strength and young's modulus of the pure PLA. It is observed that the maximum stress can be seen at 60.89 MPa, young's modulus at 776.20 MPa, and 38.47 J m^{-1} for impact strength. The quadratic model statistical testing was employed in form of Analysis of Variance (ANOVA) to obtain an optimum procedure.

As such, Table 3 shows the ANOVA results for the fitted quadratic polynomial model of pure PLA based on maximum stress responses. In Table 3, Pure-error is calculated as the square root of the sum of squared differences between the observed and the predicted values divided by the number of subjects in the cross-validation sample. The smaller the pure error, the greater the accuracy of the equation. Moreover, Lack-of-fit compares the residual error with the pure error. Corrected total (Cor. Total) value, is the total amount of variation that occurs with the individual observations of response about the mean.

Table 3. Analysis of variance for the fitted quadratic polynomial model of PLA processing (max stress).

Source	Sum of squares	Degree freedom	Mean square	*F*-value	*P*-value
Model	279.78	9	31.09	26.81	< 0.0001
Residual	9.28	8	1.16		
Lack of fit	9.28	3	3.09		
Pure error	0.00	5	0.00		
Cor. total	289.05	17			

$R^2 = 0.9679$; $R^2_{adj}=0.9318$; C.V.% = 1.96.

Model *F*-value was calculated as ratio of mean square regression and mean square residual. The *F*-value is the test for comparing the curvature variance with residual (error) variance and *P*-value is probability of seeing the observed *F*-value if the null hypothesis is true. If the null hypothesis is true, it shows that the model is a good predictor of the experimental data. Therefore, the larger *F*-value and the smaller *P*-value, corresponds to more significant coefficient.

Model *F*-value of 26.81 approved the model significant and stability (Table 3). Furthermore, model *P*-value of <0.0001 complemented the model significance, as it was less than 0.05, indicating the feasibility of using RSM strategies in this study. The model resulted in an acceptable adj. R^2 with R^2 difference value of 0.03 (values are preferred to be less than 0.2). Coefficient of variation (C.V.) percentage is a standard deviation expressed as a percentage of the mean, where the lower the C.V., the smaller residuals relative to the predicted value was. Therefore, C.V. value for the fitted quadratic polynomial model was 1.96, proposing a reliable model. Concluding equation based on coded factors was obtained from the software and presented in Equation (1).

$$\begin{aligned}\text{Maximum stress} = {} & (+57.30) - (1.22 \times A) \\ & - (4.19 \times B) - (1.00 \times C) \\ & - (2.11 \times A \times B) \\ & - (0.64 \times A \times C) \\ & - (0.86 \times B \times C) \\ & - (1.89 \times A^2) - (1.95 \times B^2) \\ & - (1.29 \times C^2). \end{aligned} \quad (1)$$

Figure 1 shows the 3D interaction plot of processing temperature, mixing speed, and duration factors with

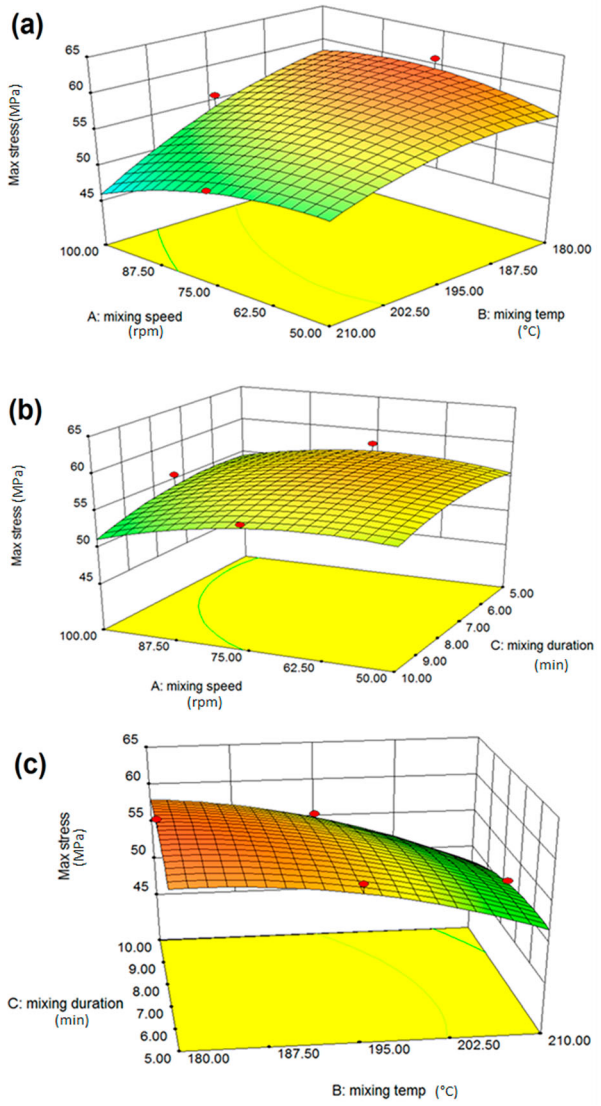

Figure 1. Response surface (3D) presenting the effect of mixing speed, mixing duration, and mixing temperature on maximum stress value.

maximum stress response. A clear decline in maximum stress value can be observed as the temperature increased to 210°C (Figure 1(a,c)). The mixing duration and speed had little influence on maximum stress value. However, as mixing speed was increased over 75 rev min^{-1} a slight decline in maximum stress was observed (Figure 1(b)).

Table 4 shows the ANOVA for the fitted quadratic polynomial model following Young's modulus (MPa) responses. From the table, *F*-value of 10.07 indeed proved the significance of the model, which was further complemented by the *P*-value of less than 0.050. Similar to the maximum stress model, Young's modulus model presented an acceptable adj. R^2 with R^2 difference value of 0.0913. From the R^2 value obtained, it can be concluded that the quadratic equation defines 91.89% of the total variation of the experimental results. A C.V. percentage of 3.55% also proved the significance of the model. The final equation in terms of coded factors based on DTG results was presented in Equation (2).

Table 4. Analysis of variance for the fitted quadratic polynomial model of PLA processing (Young's Modulus).

Source	Sum of squares	Degree freedom	Mean square	*F*-value	*P*-value
Model	38775.21	9	4308.36	10.07	0.0017
Residual	3424.23	8	428.03		
Lack of fit	3424.23	3	1141.41		
Pure error	0.000	5	0.000		
Cor. total	42199.44	17			

$R^2 = 0.9189$; $R^2_{adj} = 0.8276$; C.V.% = 3.55.

$$\begin{aligned}\text{Young's Modulus} = {} & (+537.77) + (6.73 \times A) \\ & + (7.22 \times B) + (3.57 \times C) \\ & - (16.05 \times A \times B) \\ & + (27.06 \times A \times C) \\ & + (13.35 \times B \times C) \\ & + (12.84 \times A^2) \\ & + (57.62 \times B^2) \\ & + (15.81 \times C^2) \end{aligned} \quad (2)$$

Figure 2 depicts the 3D interaction graph of the three factors with young's modulus value. Processing temperature at 190°C showed a significant effect on the young's modulus value (Figure 2(a)). Meanwhile, either higher or lower temperatures than 190°C showed to be beneficial. Likewise the previous findings, processing speed and duration appeared to have minimal effect on young's modulus values.

Table 5 shows the ANOVA fitted quadratic polynomial model for the impact strength. From the table, the model's *F*-value of 6.54 and *P*-value less than 0.050 proved the significance of the model. The coefficient of variation (C.V.% = 3.37) of the response values further illustrated that the model has high reliability. The impact strength model presented an adequate adj. R^2 with R^2 difference value of 0.0913. The overall equation based on the coded factors was presented in Equation (3).

$$\begin{aligned}\text{Impact strength} = {} & (+29.21) - (0.016 \times A) \\ & - (1.82 \times B) - (0.66 \times C) \\ & - (1.45 \times A \times B) \\ & + (0.50 \times A \times C) \\ & - (0.80 \times B \times C) \\ & - (0.49 \times A^2) - (0.42 \times B^2) \\ & + (0.14 \times C^2) \end{aligned} \quad (3)$$

Figure 3 presents the 3D interaction graphs of mixing temperature, speed, and duration interaction with impact strength value. Increase in mixing temperature from 180°C to 210°C appeared to clearly decrease the

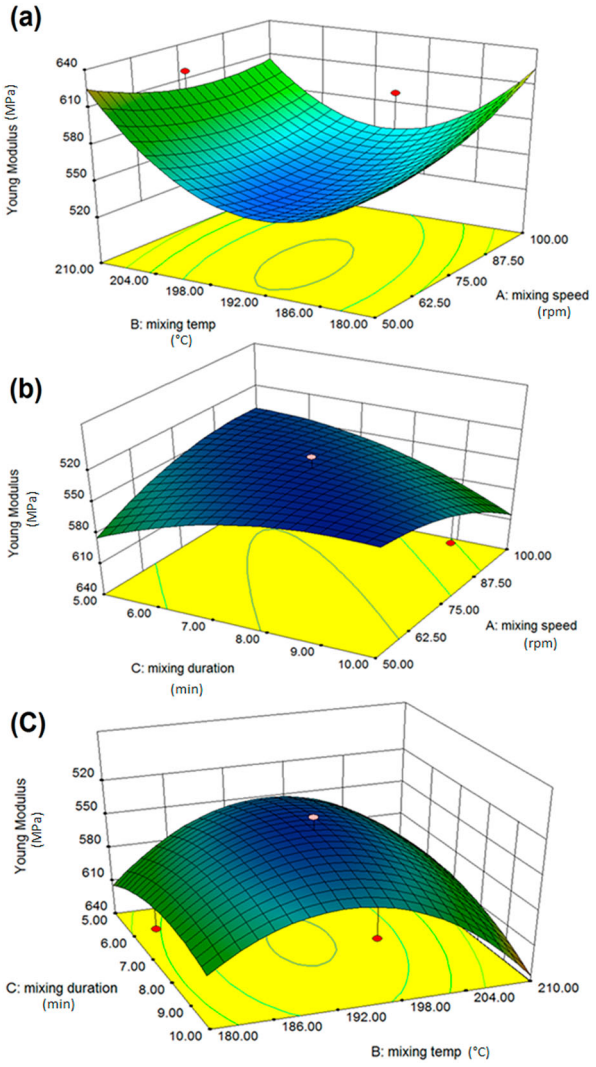

Figure 2. Response surface (3D) presenting the effect of mixing speed, mixing duration, and mixing temperature on young's modulus value.

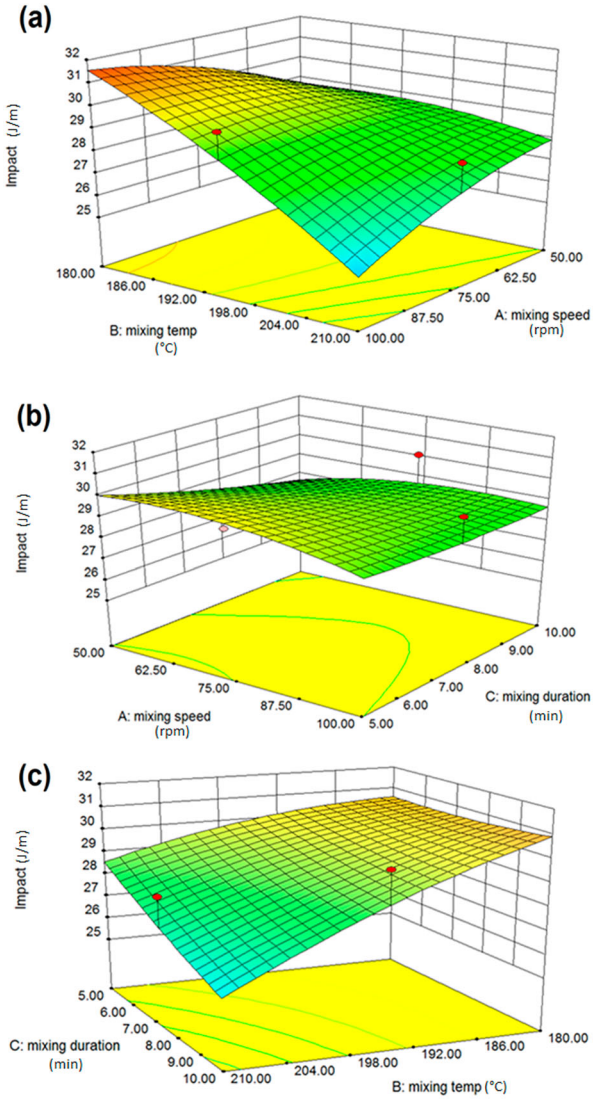

Figure 3. Response surface (3D) presenting the effect of mixing speed, mixing duration, and mixing temperature on impact strength value.

impact strength properties (Figure 3(a,b)). In the meantime, as observed earlier, mixing speed and duration appeared to have minor influence on impact properties as compared to the processing temperature.

Processing parameters optimisation

To optimise the blending parameters, the goals for mixing temperature, speed, and duration were set to 'in range'. The three responses were set to 'maximise'. This was to obtain the highest mechanical performance over the lowest processing temperature. As observed earlier, processing temperatures higher than 180°C showed less desirability. Based on this setting, the software suggested 33 solutions carrying a desirability ranged from 0.72 to 0.92. The solution with the highest desirability value of 0.92 was selected. Optimum parameters 3D diagram was presented in Figure 4.

The predicted optimised factors for the blend conditions were mixing temperature of 180°C, mixing time of 10 min and mixing speed of 100 rev min^{-1}. Moreover, the predicted responses of the blend based on these predicted factors were 56.84 MPa, 651.13 MPa, and 32.23 J m^{-1} for maximum stress, young modulus, and impact strength values accordingly. Upon validation process, actual average values of 60.31 MPa, 606.54 MPa, and 31.65 J m^{-1} for maximum stress, young modulus, and impact strength were achieved respectively. In terms of error percentage, validation results were −5.75%, 7.35%, and 1.83% for maximum stress, young modulus, and

Table 5. Analysis of variance for the fitted quadratic polynomial model of PLA processing (Impact strength).

Source	Sum of squares	Degree freedom	Mean square	*F*-value	*P*-value
Model	56.33	9	6.26	6.54	0.0072
Residual	7.65	8	0.96		
Lack of fit	7.65	3	2.55		
Pure error	0.000	5	0.000		
Cor. total	63.98	17			

$R^2 = 0.8804$; $R^2_{adj} = 0.7458$; C.V.% = 3.37.

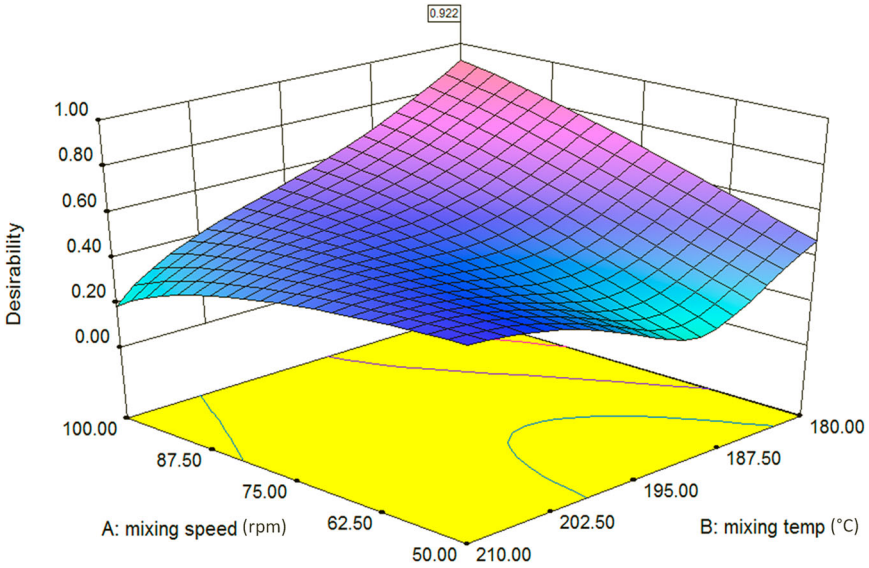

Figure 4. 3D interaction plot of optimum mixing temperature and speed.

impact strength values accordingly. Validation process resulted in a slightly higher stress value while lower in young modulus. The negative error percentage indicates the higher maximum stress validation value than the predicted value.

To further study the role of temperature, morphological studies were carried out. Figure 5 shows tensile and notched izod impact fracture surfaces of H11, H4, and H20 samples. H11, H4, and H20 samples were prepared at same condition (blended for 7.5 min at 75 rev min^{-1}) while at different temperatures (at 180°C, 195°C, 210°C respectively). During the tensile test, the failure occurs due to initiation of craze that spread catastrophically across the specimen and rapidly fractures the sample under relatively high level of stress [27]. The crazes, which dissipate the strain energy by plastic deformation, were clearly observed in Figure 5(a–e). The crazes grow in a direction perpendicular to the applied tension. It was observed that the fracture behaviour of the specimens in the tensile test changed from ductile fracture to brittle fracture with increasing the temperature from 180°C to 210°C. A large amount of energy consumed in craze development is the major source of toughness. The samples prepared at a higher

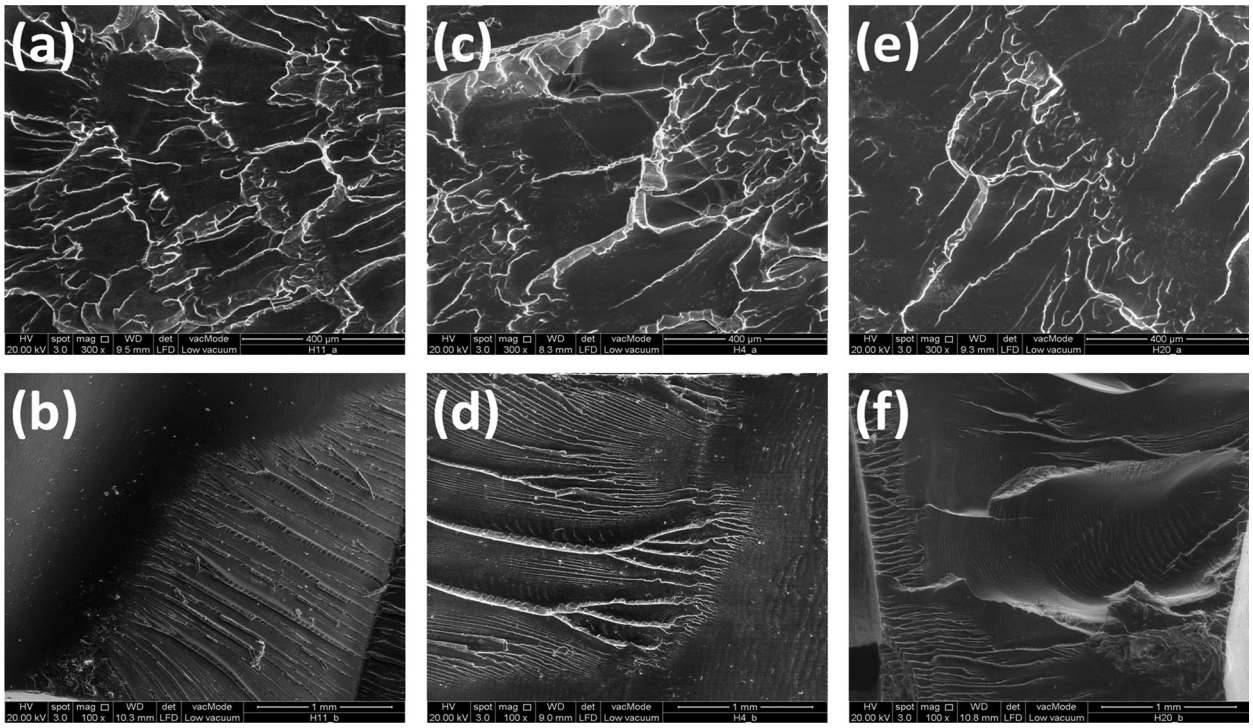

Figure 5. Morphological structure of H11 ((a) Tensile, (b) Impact), H4 ((c) Tensile, (d) Impact), and H20 ((e) Tensile, (f) Impact) samples.

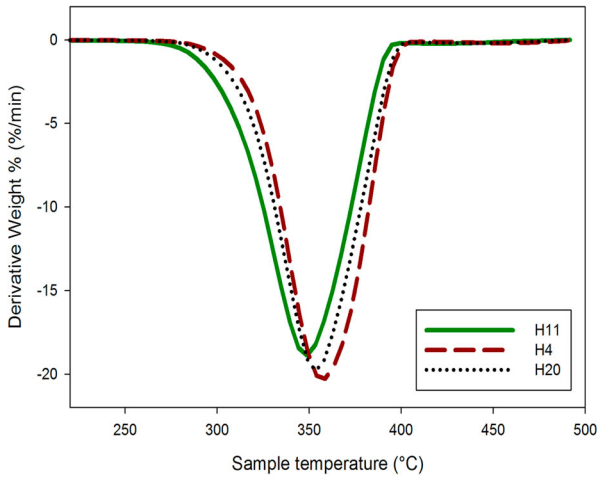

Figure 6. DTG thermogram results of H11, H4, and H20 samples.

temperature than 180°C, had relatively lower mechanical strength which was linked to the reduction in number of crazes and increasing brittleness of specimens. Similarly, the fracture surfaces of impact results show the transition to a more brittle structure at higher temperatures (Figure 5(b,d,f)). The flexural ductility of H4 and H20 decreased and their stiffness increased with increasing temperature.

In addition to morphological characterisation, thermal analysis was carried out to further understand the influence of processing temperature. Similarly, H11, H4, and H20 samples were selected. Figure 6 presents the effect of processing temperature on the thermal stability of the PLA. PLA is thermally unstable and exhibits rapid loss of molecular weight as the result of thermal treatment at processing temperatures. The ester linkages of PLA tend to degrade during thermal processing or under hydrolytic conditions. To further study the thermal stability of H11, H4, and H20, different thermal degradation stages as a function of temperature were analysed (Table 6). The temperatures T_5, T_{10}, T_{50}, T_{max} and T_{90} are temperatures for 5%, 10%, 50%, maximum and 90% decomposition, respectively. Higher the values of T_5, T_{10}, T_{50}, T_{max} and T_{90}, higher will be the thermal stability of the sample. T_{max} of H11 which was prepared at 180°C was at ~348°C while H4 and H20 which were processed at higher temperatures were at ~359°C and ~353°C respectively. Thermal degradation mainly occurs through random main-chain scissions coupled with other reactions such as hydrolysis, depolymerisation, oxidative degradation, and inter and intramolecular trans-esterification reactions to mononmer and oligomeric esters [28].

Moreover, the transparent light yellow colour of the samples blended at 180°C was changed to darker brownish colour for the samples processed at 210°C. The change in colour also confirms the degradation of the polymer at higher temperatures [28].

Table 6. Thermal stability data of H4, H11, and H20 obtained from TGA curves.

	TGA				
Sample	T_5 (°C)	T_{10} (°C)	T_{50} (°C)	T_{max} (°C)	T_{90} (°C)
H11 (180 °C)	307.75	318.32	349.25	348.07	362.64
H4 (195°C)	322.34	333.96	359.07	359.44	370.82
H20 (210°C)	317.55	328.55	354.59	353.61	367.18

Conclusion

Maximum preparation temperature of pure PLA was investigated using a statistic model. A range of temperature starting from 180°C to 210°C was selected. It was observed that process temperature plays the most important role as compared to mixing duration and speed. Samples prepared at higher temperatures than 180°C presented lower mechanical properties while having smoother structure. Moreover, the quadratic polynominal model showed to be suitable to optimise preparation parameters. The optimal blending condition for PLA was obtained at 180°C, 10 min and 100 rev min^{-1}. Validation process confirms the optimal predicted values. The optimised parameters resulted in maximum stress, young modulus, and impact strength values of 60.31 MPa, 606.54.54 MPa, and 31.65 J m^{-1} respectively. To obtain an acceptable mechanical performance, preparation of PLA composites at temperatures higher than 180°C is not recommended.

Disclosure statement

No potential conflict of interest was reported by the authors.

References

[1] Tharanathan RN. Biodegradable films and composite coatings: past, present and future. Trends Food Sci Technol. 2003;14(3):71–78. http://www.sciencedirect.com/science/article/pii/S0924224402002807.

[2] Dong P, Prasanth R, Xu F, et al. Eco-friendly polymer Nanocomposite—properties and processing. In: Thakur VK, Thakur MK, editors. Advanced Structured materials. NY: Springer; 2015. p. 1–15. Eco-friendly Polymer Nanocomposites Chap. 1.

[3] Genovese L, Lotti N, Gazzano M, et al. Novel biodegradable aliphatic copolyesters based on poly (butylene succinate) containing thioether-linkages for sustainable food packaging applications. Polym Degrad Stab. 2016;132:191–201.

[4] Jabeen N, Majid I, Nayik GA, et al. Bioplastics and food packaging: A review. Cogent Food Agric. 2015;1(1):1117749.

[5] Wang Y-n, Weng Y-x, Wang L. Characterization of interfacial compatibility of polylactic acid and bamboo flour (PLA/BF) in biocomposites. Polym Test. 2014;36:119–125.

[6] Auras R, Harte B, Selke S. An overview of polylactides as packaging materials. Macromol Biosci. 2004;4 (9):835–864.
[7] Devi RS, Kannan VR, Natarajan K, et al. The role of Microbes in plastic degradation. Chap. 12. In: Ram Chandra, editor. Environmental Waste Management. UK: Taylor & Francis; 2015. p. 341–370.
[8] Soroudi A, Jakubowicz I. Recycling of bioplastics, their blends and biocomposites: A review. Eur Polym J. 2013;49(10):2839–2858.
[9] Reddy MM, Vivekanandhan S, Misra M, et al. Biobased plastics and bionanocomposites: Current status and future opportunities. Prog Polym Sci. 2013;38 (10–11):1653–1689. http://www.sciencedirect.com/science/article/pii/S0079670013000476.
[10] Garlotta D. A literature review of poly (lactic acid). J Polym Environ. 2001;9(2):63–84.
[11] Dong Y, Ghataura A, Takagi H, et al. Polylactic acid (PLA) biocomposites reinforced with coir fibres: evaluation of mechanical performance and multifunctional properties. Compos Part A: Appl Sci Manuf. 2014;63:76–84.
[12] Datta R, Henry M. Lactic acid: recent advances in products, processes and technologies—a review. J Chem Technol Biotechnol. 2006;81(7):1119–1129.
[13] Chieng BW, Ibrahim NA, Then YY, et al. Mechanical, thermal, and morphology properties of poly(lactic acid) Plasticized With poly(ethylene glycol) and Epoxidized Palm Oil Hybrid plasticizer. Polym Eng Sci. 2016, doi:10.1002/pen.24350.
[14] Chieng BW, Ibrahim NA, Then YY, et al. Plasticized and Nanofilled poly (lactic acid) Nanocomposites: mechanical, thermal and morphology properties. Mater Sci Forum. 2016;846:429–433.
[15] Mehta R, Kumar V, Bhunia H, et al. Synthesis of poly (lactic acid): a review. J Macromol Sci Part C: Polym Rev. 2005;45(4):325–349.
[16] Ketabchi MR, Hoque ME, Siddiqui MK. Critical Concerns on Manufacturing processes of natural Fibre Reinforced polymer composites. Chap. 6. In: Mohd Sapuan Salit, Mohammad Jawaid, Nukman Bin Yusoff, et al., editors. Manufacturing of natural Fibre Reinforced polymer composites. NY: Springer; 2015.
[17] Kong I, Tshai K, Hoque ME. Manufacturing of natural Fibre-Reinforced polymer composites by solvent casting method. Chap. 16. In: Mohd Sapuan Salit, Mohammad Jawaid, Nukman Bin Yusoff, et al., editors. Manufacturing of natural Fibre Reinforced polymer composites. Ny: Springer; 2015.
[18] Bulota M, Budtova T. PLA/algae composites: morphology and mechanical properties. Compos Part A: Appl Sci Manuf. 2015;73:109–115. http://www.sciencedirect.com/science/article/pii/S1359835X15000809.
[19] Herrera N, Salaberria AM, Mathew AP, et al. Plasticized polylactic acid nanocomposite films with cellulose and chitin nanocrystals prepared using extrusion and compression molding with two cooling rates: effects on mechanical, thermal and optical properties. Compos Part A: Appl Sci Manuf. 2016. http://www.sciencedirect.com/science/article/pii/S1359835X15001852.
[20] Yang X, Clénet J, Xu H, et al. Two Step extrusion process: from thermal Recycling of PHB to Plasticized PLA by Reactive extrusion Grafting of PHB degradation Products onto PLA Chains. Macromolecules. 2015;48(8):2509–2518. doi:10.1021/acs.macromol.5b00235.
[21] Fox DM, Novy M, Brown K, et al. Flame retarded poly (lactic acid) using POSS-modified cellulose. 2. effects of intumescing flame retardant formulations on polymer degradation and composite physical properties. Polym Degrad Stab. 2014;106:54–62. http://www.sciencedirect.com/science/article/pii/S0141391014000093.
[22] Asaithambi B, Ganesan G, Ananda Kumar S. Bio-composites: development and mechanical characterization of banana/sisal fibre reinforced poly lactic acid (PLA) hybrid composites. Fibers Polym. 2014;15(4):847–854. doi:10.1007/s12221-014-0847-y.
[23] Robles E, Urruzola I, Labidi J, et al. Surface-modified nano-cellulose as reinforcement in poly(lactic acid) to conform new composites. Ind Crops Prod. 2015;71:44–53. http://www.sciencedirect.com/science/article/pii/S0926669015002654.
[24] Nair PP, George KE, Jayakrishnan N. Studies on mechanical behavior high impact polystyrene/vinyl clay nanocomposites: Comparison between in situ polymerization and melt mixing. Polym Compos. 2015. doi:10.1002/pc.23561.
[25] Rasyid MA, Salim M, Akil H, et al. Optimization of processing conditions Via response surface methodology (RSM) of Nonwoven Flax Fibre Reinforced Acrodur Biocomposites. Procedia Chem. 2016;19:469–476.
[26] Daneshpayeh S, Ashenai Ghasemi F, Ghasemi I, et al. Predicting of mechanical properties of PP/LLDPE/TiO2 nano-composites by response surface methodology. Compos Part B: Eng. 2016;84:109–120. http://www.sciencedirect.com/science/article/pii/S1359836815005156.
[27] Grijpma DW, Pennings AJ. (Co) polymers of L-lactide, 2. mechanical properties. Macromol Chem Phys. 1994;195(5):1649–1663.
[28] Pradhan S, Chakraborty I, Kar B. Chemically modified Lignin–A Potential Resource material For composites With Better stability. Int J Sci Environ. 2015;4 (1):183–189.